ChemPubSoc Europe

DOI: 10.1002/chem.201405381

CHEMISTRY A European Journal Full Paper

Pi Interactions

Design of Aromatic-Containing Cell-Penetrating Peptide Mimics with Structurally Modified π Electronics

Brittany M. deRonde,[a] Alexander Birke,[a] and Gregory N. Tew*[a, b]

Abstract: Cell-penetrating peptides (CPPs) and their synthetic mimics (CPPMs) represent a class of molecules that facilitate the intracellular delivery of various cargo. Previous studies indicated that the presence of aromatic functionalities improved CPPM activity. Given that aromatic functionalities play prominent roles in membrane biology and participate in various π interactions, we explored whether these interactions could be optimized for improved CPPM activity. CPPMs were synthesized by ring-opening metathesis polymerization by using monomers that contained aromatic rings substituted with electron-donating and electron-withdrawing groups and covered an electrostatic potential range from −29.69 to +15.57 kcal mol^{-1}. These groups altered the quadrupole moments of the aromatic systems and were used to test if such structural modifications changed CPPM activity. CPPMs were added to dye-loaded vesicles and the release of carboxyfluorescein was monitored as a function of polymer concentration. Changes in the effective polymer concentration to release 50% of the dye (effective concentration, EC_{50}) were monitored. Results from this assay showed that the strength of the electron-donating and electron-withdrawing groups incorporated in the CPPMs did not alter polymer EC_{50} values or activity. This suggests that other design parameters may have a stronger impact on CPPM activity. In addition, these results indicate that a wide range of aromatic groups can be incorporated without negatively impacting polymer activity.

Introduction

Cell-penetrating peptides (CPPs) and their synthetic mimics (CPPMs) represent a unique class of molecules that is capable of crossing biological membranes.[1] The peptides are generally short, cationic sequences rich in arginine and/or lysine residues, with some containing hydrophobic residues such as leucine, phenylalanine, or tryptophan.[1b,g,i,j] They derive inspiration from proteins with translocation abilities, such as HIV-1 Tat and *antennapedia* homeodomain protein.[2] It has been shown that the cation-rich domains of these proteins, referred to as protein-transduction domains (PTDs), are primarily responsible for their uptake abilities.[2a,3] Many studies have highlighted the ability of CPP(M)s to facilitate the intracellular delivery of various cargo, including, but not limited to, small molecules, siRNA, pDNA, and proteins by covalent or non-covalent interactions.[1b,c,e,g–j,4] Although their mechanism of uptake is debated in the literature, various forms of endocytosis, macropinocytosis, protein-dependent translocation, and energy-independent translocation are involved in the internalization process.[5]

In efforts to elucidate the mechanisms of CPP(M) uptake and assess the structural components of CPP(M)s necessary for uptake, model vesicle membrane studies have frequently been used.[6] Vesicle experiments represent a simpler system for evaluating energy-independent methods of transduction than using cells, in which it is difficult to decouple various methods of cellular uptake. Previously, Matile and co-workers have used model vesicle systems to show that polyarginine, a widely used CPP, requires hydrophobic counterions to efficiently cross lipid membranes.[6b,7] For these studies, lipids were swollen in a solution of carboxyfluorescein, which is a hydrophilic, anionic dye that self-quenches at high concentrations, and dye release was monitored as a function of peptide concentration. Changes in peptide activity were assessed by calculating the effective concentrations to release 50% of the dye (effective concentration, EC_{50}). Similar assays have also been used by Almeida and co-workers to explore CPP internalization mechanisms.[8] The hydrophobic counterions selected for Matile and co-workers studies were said to help mask the overall cationic charge of the peptides to aid in transduction, a process referred to as activation.[6b,7] Although these studies showed that bulky aromatic activators, such as pyrene butyrate, outperformed aliphatic activators, the roles of hydrophobicity and aromaticity were not fully understood.

Motivated by these studies, our lab previously developed a series of oxanorbornene imide-based CPPMs to assess the effect of hydrophobicity on CPPM activity.[6d,e] Instead of using external activators, the hydrophobic components were chemi-

[a] *B. M. deRonde, A. Birke, Prof. G. N. Tew*
Department of Polymer Science & Engineering
University of Massachusetts, Amherst, MA 01003 (USA)
Fax: (+1) 413-545-0082
E-mail: tew@mail.pse.umass.edu

[b] *Prof. G. N. Tew*
Department of Veterinary and Animal Sciences
Molecular and Cellular Biology Program
University of Massachusetts, Amherst, MA 01003 (USA)

Supporting information for this article is available on the WWW under http://dx.doi.org/10.1002/chem.201405381. It contains all experimental details.

cally incorporated into the polymeric structures to give self-activating polymers.[6d,e] These polymers were correctly predicted to outperform their counterparts that only contained cationic residues.[6a,d,e] Initially, various aliphatic chains were incorporated into the CPPMs to assess the effect of chain length on activity.[6e] These results were evaluated by assessing differences in reported EC_{50} values from vesicle dye release assays.[7b] Although polymer activity improved by increasing the alkyl chain lengths from one carbon to four carbons, longer alkyl chains were less water soluble and thus led to poorer performance.[6e]

Another series of polymers was designed to evaluate the impact of various aromatic, cyclic non-aromatic, and alkyl hydrophobic moieties of similar hydrophobicity on polymer activity.[6d] This was done to gain a better understanding of the interplay between hydrophobicity and aromaticity. Aromaticity was the cornerstone of that report because of the significant role it plays in protein–membrane interactions. The aromatic amino acids tyrosine and tryptophan are present as part of aromatic belts that flank either end of transmembrane proteins.[9] These residues sit at the interface between the hydrophobic core and the more hydrophilic external environment to enhance stability at those regions.[9] Although not typically present in aromatic belts, phenylalanine has also been shown to aid in anchoring proteins in the membrane.[10] All three of these aromatic amino acids have been shown to provide favorable energies of insertion into membranes.[10] It was further reasoned that aromatic moieties are ideal for incorporation into CPPMs because such residues are found in many CPPs, including Penetratin, Pep-1, and MPG, and have been shown in some cases to be critical for uptake.[1e,11] Experiments, in which aromatic residues in Tat and Penetratin were replaced with non-aromatic hydrophobic residues, led to a reduction in cellular internalization efficiencies.[1e,11]

Using HPLC retention times to assess relative hydrophobicity of the polymer side chains,[12] these values were compared to the polymer EC_{50} values to illustrate that the effects of hydrophobicity and aromaticity could be distinguished. Through these studies, it was suggested that aromatic hydrophobic moieties were superior activators.[6d] Similar results were obtained by Matile and co-workers when they monitored dye release of polyarginine with various external activators.[7d]

Given these observations and the different electronic properties of tyrosine, phenylalanine, and tryptophan (Figure S1 and Table S1 in the Supporting Information), the role of aromaticity in CPP(M) activity was studied by exploring the effect that changes in quadrupole moments have on these systems. The flat, planar structures of these aromatic rings and their associated quadrupole moments are thought to enable various π interactions, such as π–π, π cation, π anion, and π polar interactions within the cellular environment that can aid in membrane interactions.[10a,13] Because the quadrupole moment collects the electron density on the face of these planar, aromatic rings, it was hypothesized that by strengthening or weakening this phenomenon, the corresponding π membrane interactions would provide additional handles for tuning of CPPM activity. Specifically, this was attempted by incorporating electron-donating and electron-withdrawing groups into the aromatic systems as a way to alter the electron density of the ring system. Although nature offers an electrostatic potential range for its aromatic amino acids between −31.41 (Trp) and −23.48 kcal mol^{-1} (Tyr), by using synthetic systems, it was possible to examine a much wider electrostatic potential window of −29.69 kcal mol^{-1} (Scheme 1, R = b = CH_3) to +15.57 kcal mol^{-1} (Scheme 2, R′ = c = NO_2). All values are summarized in Table S1–2 in the Supporting Information.

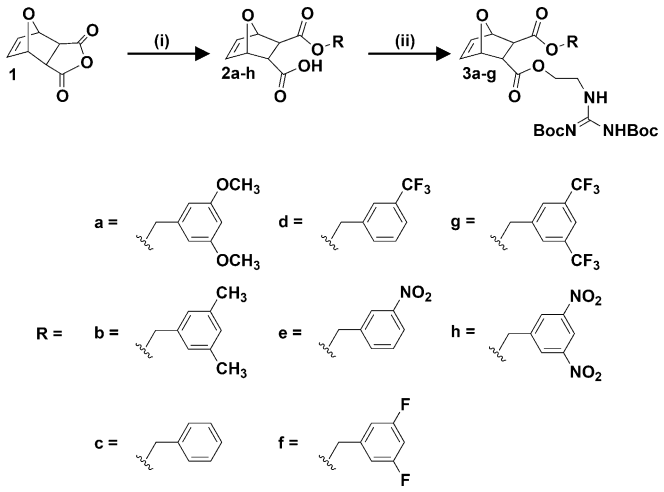

Scheme 1. Synthesis of diester monomers containing π-rich and π-poor aromatic rings. i) R–OH, DMAP, CH_2Cl_2, RT, overnight; ii) 1,3-di-Boc-2-(2-hydroxyethyl)guanidine, EDC, DMAP, CH_2Cl_2, 0 °C to RT, overnight.

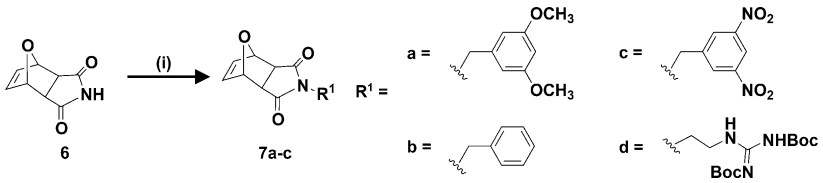

Scheme 2. Synthesis of imide monomers containing π-rich and π-poor aromatic rings. i) R^1–OH, PPh_3, diisopropyl azodicarboxylate (DIAD), THF, RT, 18 h.

As part of this study, π-rich and π-poor CPPMs were designed and synthesized based on both the diester and imide ROMP scaffolds. CPPMs based on the diester system were synthesized because the dual-functional monomers offer greater potential for polymeric structure variations. Also, CPPMs based on the imide scaffold were synthesized as a direct comparison to polymers from previous hydrophobicity structure activity relationships (SARs) with model membranes.[6d,e] These CPPMs were designed to contain π-rich and π-poor aromatic functionalities to assess the role of π interactions in tuning membrane activity.

Results and Discussion

Monomer synthesis

Diester monomers were synthesized by using a two-step process (Scheme 1). These procedures were adapted from previously described methods with modifications.[4a,14] In brief, oxanorbornene anhydride (**1**) was ring opened by using various aromatic alcohols (**a**–**h**) and 4-dimethylaminopyridine (DMAP) to give the half-ester intermediates.

Half-esters **2a**–**f** were then further reacted with 1,3-di-boc-2-(2-hydroxyethyl)guanidine by using 1-ethyl-3-(3-dimethylaminopropyl)carbodiimide (EDC)-coupling conditions to give monomers **3a**–**f**. Half-esters **2g**–**h** were not used for monomer synthesis, because they proved to be unstable in solution at room temperature. As shown in Figure 1A, half-esters **2g**–**h** underwent a spontaneous retro-Diels–Alder reaction to yield **4g**–**h** and furan (**5**). This was demonstrated by isolating the retro-Diels–Alder product, **4g**, using column chromatography and verifying its chemical composition by using ^{1}H NMR, ^{13}C NMR, and mass spectrometry (MS). Retro-Diels–Alder product **4h** proved to be more difficult to isolate because of additional nitro-based impurities.

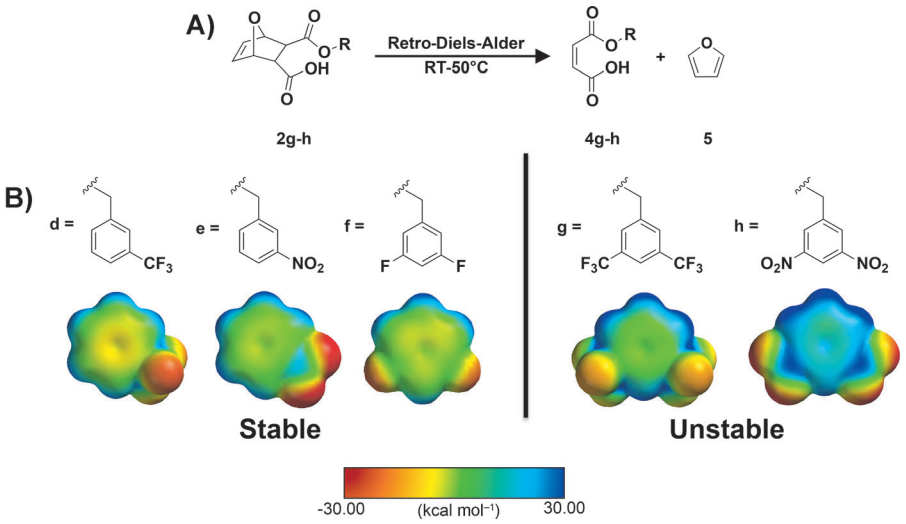

Figure 1. Stability of π-poor monomers. A) Retro-Diels–Alder reaction that occurs for monomers **4g**–**h**. B) Stable and unstable π-poor monomer aromatic groups with their corresponding electrostatic potential maps. The range for electrostatic potential was set between −30.00 and 30.00 kcal mol^{-1}. The color scale bar reflects this range with red representing electron-rich surfaces, and blue representing electron-poor surfaces. Surfaces were calculated at the HF level by using the 3-21G* basis set.[17]

However, peaks for the retro-Diels-Alder product were observed in the ^{1}H NMR of **2h** (see the Supporting Information). Because **2a**–**f** did not appear to undergo the retro-Diels–Alder reaction, it was hypothesized that this reaction was related to the electron-withdrawing substituents attached to the aromatic rings. To investigate this, all π-poor aromatic rings were modeled using Spartan molecular modeling software[17] as shown in Figure 1B. The most electron-poor (most blue in color) aromatic rings were the rings associated with the unstable half esters. From this and a study by Nanjappan and Czarnik, it was concluded that electron-withdrawing groups destabilized Diels–Alder adducts and accelerated the retro-Diels–Alder reaction.[15]

Compounds **2g**, **h** were not pursued for monomer formation because the retro-Diels–Alder impurities **4g**,**h** have the same reactive functional groups (–COOH, C=C) as **2a**–**f**. All stable half-esters and monomers were characterized by ^{1}H NMR, ^{13}C NMR spectroscopy, and MS. In terms of electrostatic potential values, the six stable monomers covered an electrostatic potential range from −4.66 kcal mol^{-1} (Scheme 1, R = e = NO_2) to +29.69 kcal mol^{-1} (Scheme 1, R = b = CH_3). Electrostatic potential values are summarized in Table S2 in the Supporting Information; all characterization data is provided in the Supporting Information.

Imide monomers were synthesized by using a one-step process adapted from Som et al, as illustrated in Scheme 2.[6d,e] Unlike the diester system, there were no issues with stability for the imide system, and no retro-Diels–Alder products were observed. All monomers were characterized by ^{1}H NMR, ^{13}C NMR techniques, and MS. In terms of electrostatic potential values for the aromatic groups incorporated, all stable monomers covered an electrostatic potential range from −18.10 kcal mol^{-1} (Scheme 2, R^1 = a = OCH_3) to 15.57 kcal mol^{-1} (Scheme 2, R^1 = c = NO_2). These monomers expand the negative end of the electrostatic potential range so that in total the monomer design spans −29.69 to +15.57 kcal mol^{-1} as summarized in Table S2 in the Supporting Information.

Polymer Synthesis

Polymers were synthesized by using ROMP with Grubbs third-generation catalyst, as illustrated in Schemes 3, 4, and 5.

All *tert*-butyloxycarbonyl (Boc)-protected polymers (**8a**–**f**, **10a**–**c**, **13a**,**c**,**e**) were characterized by ^{1}H NMR to assess chemical composition and gel-permeation chromatography (GPC) to assess relative molecular weights. GPC data are summarized in Table 1.

Polymers were subsequently deprotected using trifluoroacetic acid (TFA) and CH_2Cl_2 (1:1) overnight.[4a,6d,e,14] TFA was removed by azeotropic distillation with methanol. Diester polymers were dialyzed for three days in water by using membranes with a molecular weight cut-off of 2000 g mol^{-1} for homopolymers and 1000 g mol^{-1} for random copolymers. All polymers were then dissolved in water and lyophilized to yield dry **9a**–**f**, **12a**–**c**, and **15a**,**c**,**e**.

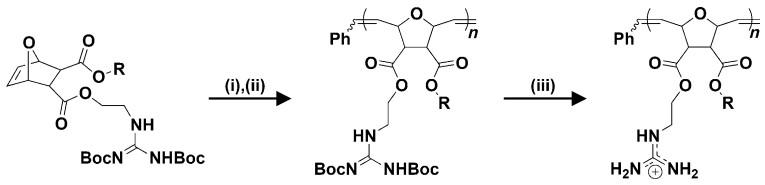

Scheme 3. Synthesis of diester homopolymers containing π-rich and π-poor aromatic rings. i) Dichloro-di(3-bromopyridino)-*N*,*N*′-dimesitylenoimidazolino–Ru=CHPh (G3) catalyst, CH_2Cl_2, RT, 45 min; ii) ethyl vinyl ether, RT, overnight; iii) TFA/CH_2Cl_2 (1:1), RT, overnight. Products **9a–f** were further purified by dialysis with molecular weight cut-off 2000 g mol^{-1}. All polymers were synthesized with $n=20$; R is defined in Scheme 1.

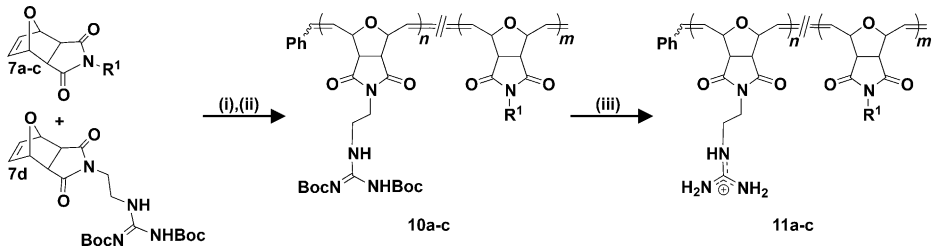

Scheme 4. Synthesis of imide random copolymers containing π-rich and π-poor aromatic rings. i) Dichloro-di(3-bromopyridino)-*N*,*N*′-dimesitylenoimidazolino–Ru=CHPh (G3) catalyst, CH_2Cl_2, RT, 45 min; ii) ethyl vinyl ether, RT, overnight; iii) TFA/CH_2Cl_2 (1:1), RT, overnight. All polymers were synthesized with $n=20$ and $m=20$; R^1 is defined in Scheme 2.

Table 1. Molecular characteristics of π-rich and π-poor CPPMs.

Diester homopolymers			Imide and diester random copolymers			
CPPM	M_n[a]	$Đ$[a]	CPPM	n/m[b]	M_n[a]	$Đ$[a]
8a	11600	1.05	**11a**	56:44	16200	1.06
8b	11200	1.05	**11b**	55:45	13700	1.07
8c	11300	1.05	**11c**	58:42	17000	1.06
8d	12600	1.05	**14a**	38:62	10600	1.10
8e	11400	1.05	**14c**	40:60	12100	1.08
8f	11500	1.05	**14e**	39:61	10700	1.14

[a] Number average molecular weight (M_n) and polydispersity indices ($Đ=M_w/M_n$) determined by GPC by using polymethyl methacrylate (PMMA) standards for diester polymers, and polystyrene standards for the imide polymers using THF as the eluent and toluene as the flow marker. [b] Ratio of residues, in which *n* represents the percentage of hydrophobic residues and *m* represents the percentage of guanidine-containing residues.

Biophysical Characterization

All polymers were tested by using a vesicle dye-release assay to assess relative polymer activity by using a fluorescence plate reader.[6a,6c–e] This high-throughput screening method enabled the testing of all samples in a 12-well plate at the same time. Carboxyfluorescein (CF)-filled phosphatidylcholine (PC) or PC/phosphatidylserine (PS) vesicles were prepared as described in the Supporting Information and then used for these experiments.

For this dye release assay, the baseline fluorescence (F_0) of 2-amino-2-hydroxymethyl-propane-1,3-diol (Tris) saline buffer with CF-filled vesicles was determined. Then, polymer solutions (in DMSO) of varying concentrations were added to the vesicle-containing solutions. After ten minutes, the fluorescence intensity ($F_{f,0}$) was measured again. Triton X-100 (5% in DMSO) was then added to each experimental solution to lyse the vesicles and release all of the dye. The final fluorescence measurement (F_t) was taken after five minutes. Complete experimental details for these experiments can be found in the Supporting Information, Figure S18. The results were normalized according to the baseline and Triton controls to yield fractional dye release (I_f) according to Equation (1):

$$I_f = (F_{f,0}-F_0)/(F_t-F_0) \quad (1)$$

For Hill analysis, I_f was plotted against polymer concentration, *c*, and fit to the Hill equation, Equation (2), to give the EC_{50}, in which I_{fr0} and I_{frmax} are the minimum and maximum value of I_f obtained for each well, respectively:

$$I_f = I_{fr0} + (I_{f,max}-I_{f,0})/[(1+c/EC_{50})^n] \quad (2)$$

The first set of polymers tested were **9a–f** and **12a–c**, because both sets of polymers had comparable hydrophobic and

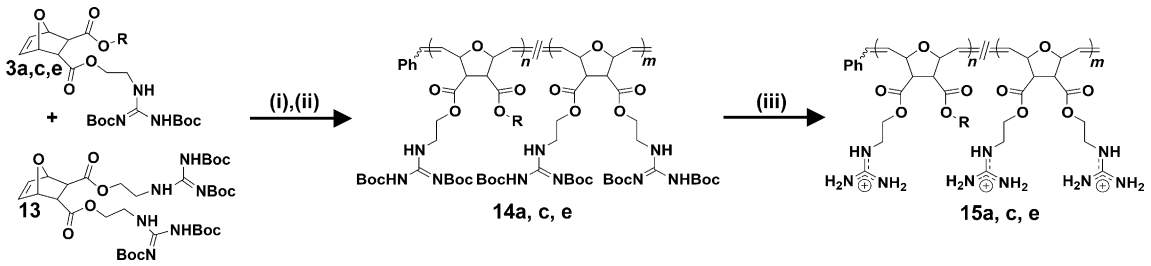

Scheme 5. Synthesis of diester random copolymers containing π-rich and π-poor aromatic rings. i) Dichloro-di(3-bromopyridino)-*N*,*N*′-dimesitylenoimidazolino–Ru=CHPh (G3) catalyst, CH_2Cl_2, RT, 45 min; ii) ethyl vinyl ether, RT, overnight; iii) TFA/CH_2Cl_2 (1:1), RT, overnight. Products **15a**,**c**, and **e** were further purified by dialysis with molecular weight cut-off:1000 g mol^{-1}. All polymers were synthesized with $n=8$ and $m=12$; R is defined in Scheme 1.

hydrophilic contents (ca. 1:1) but different backbone compositions. A summary of the EC_{50}, $I_{f,max}$, and n values obtained from testing **9a–f** and **12a–c** with PC vesicles are displayed in Table 2.

Table 2. EC_{50}, Y_{max}, and Hill coefficient n values for diester homopolymer and imide random copolymer-based CPPM activity by using 100 nm PC large unilamellar vesicles swelled with carboxyfluorescein.

CPPM	EC_{50}[a] [nM]	Y_{max}[b]	n[c]
9a	8.27±0.84	0.89±0.00	2.01±0.04
9b	7.36±1.87	0.92±0.02	1.59±0.04
9c	9.07±0.79	0.90±0.01	1.93±0.02
9d	7.48±0.50	0.91±0.01	1.43±0.01
9e	9.93±0.50	0.92±0.02	1.50±0.06
9f	8.63±0.52	0.85±0.02	1.79±0.01
12a	10.09±1.96	0.87±0.01	1.59±0.07
12b	11.85±0.19	0.84±0.05	1.63±0.14
12c	10.64±0.21	0.72±0.02	1.93±0.15

[a] EC_{50} needed to reach $Y_{max}/2$. [b] Maximum fraction of carboxyfluorescein released compared to total dye released upon addition of Triton-X 100. [c] Value n is the Hill coefficient. Standard deviation from three independent experiments is reported.

In addition, representative overlays of π-rich and π-poor polymers from both sets of polymers are shown in Figure 2. All EC_{50} values were similar (7–12 nM) and, with the exception of the lower $I_{f,max}$ for **12c**, the Hill plots were also almost identical. Only EC_{50} values that differ over several orders of magnitude represent significant changes, as was observed in previous studies, in which the aliphatic hydrophobic group incorporated was changed from a methyl group (EC_{50} = 6.4 μM) to a butyl group (EC_{50} = 0.003 μM).[6e]

Within each series, it was determined that the nature of the π-rich or π-poor aromatic rings incorporated did not have a significant impact on CPPM activity. By comparing CPPMs from both series, it was determined that the nature of the CPPM backbone also had a negligible effect on CPPM activity. Although many of our previous SAR studies were based on the imide system, in this paper all further testing was conducted with the diester system because backbone architecture had little impact on results and this system offers more options for structural tuning.

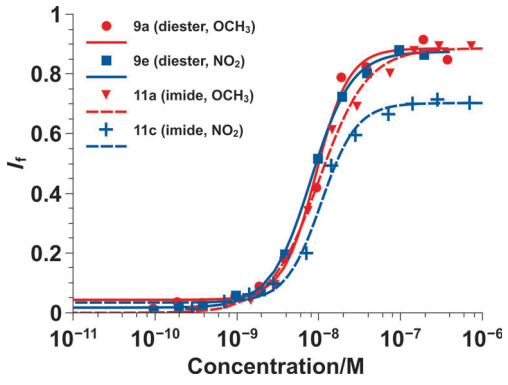

Figure 2. Diester versus imide Hill plots for π-rich CPPMs **9a** and **12a** (red) and π-poor CPPMs **9e** and **12c** (blue) by using 100 nm PC large unilamellar vesicles swelled with carboxyfluorescein. Data was fit to the Hill Equation, and I_f represents the fraction of dye released. Solid lines represent diester-based CPPMs, and dashed lines represent imide random copolymer-based CPPMs.

To further probe the effect of π electronics on CPPM activity, dye-swelled vesicles were prepared by adding negatively charged PS lipids (20 mol%) to PC lipids. This lipid composition was selected to exploit potentially favorable π-anion interactions that can occur between anionic lipids and electron-deficient aromatic systems, while also capitalizing on electron repulsions between anionic lipids and electron-rich aromatic systems.[16] Based on the nature of π interactions, it was anticipated that CPPM activity would trend based on π-electron density, with π-poor CPPMs exhibiting better activity due to favorable π-anion interactions. In contrast, π-rich polymers were expected to have weaker activity due to electron repulsion between the anionic lipids and the electron-rich aromatic rings. For these studies, polymers **9a**, **c**, and **e** were tested, and the results were compared to those obtained for PC vesicles. A summary of the EC_{50}, $I_{f,max}$, and n values can be found in Table S3 in the Supporting Information. In addition, representative overlays of π-rich and π-poor polymers tested with PC and PC/PS vesicles can be found in Figure 3. EC_{50} values for polymers **9a, c**, and **e** tested with PC/PS vesicles were similar to those obtained from studies with PC vesicles. There was also little difference in the Hill plots for these polymers, regardless of the nature of the π-rich or π-poor aromatic ring incorporated or type of vesicles used for the study.

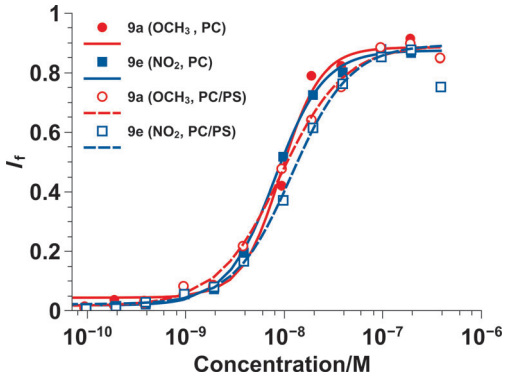

Figure 3. Anionic versus zwitterionic vesicle Hill plots for π-rich polymer **9a** (red) and π-poor polymer **9e** (blue) using two types of 100 nm large unilamellar vesicles swelled with carboxyfluorescein: PC (solid lines) and PC/PS (80:20, dashed lines). Data was fit to the Hill Equation. I_f represents the fraction of dye released.

Based on these results, a set of diester random copolymers was designed that had a more dilute hydrophobic content to make sure that the results observed were not due to the CPPM hydrophobic content being too high. The CPPMs designed are shown in Scheme 4. A summary of the EC_{50}, $I_{f,max}$, and n values can be found in Table S4 for PC and Table S5 in the Supporting Information for PC/PS vesicles. In addition, representative overlays for the diester random copolymers as they

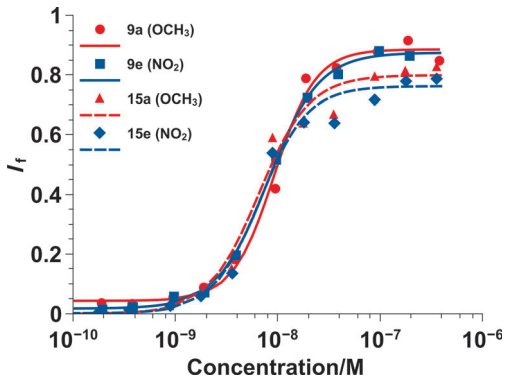

Figure 4. Homopolymer versus random copolymer Hill plots for π-rich polymers **9a** and **15a** (red) and π-poor polymers **9e** and **15e** (blue) using 100 nm PC large unilamellar vesicles swelled with carboxyfluorescein. Data was fit to the Hill Equation, and I_f represents the fraction of dye released. Solid lines represent diester homopolymers, and dashed lines represent diester random copolymers.

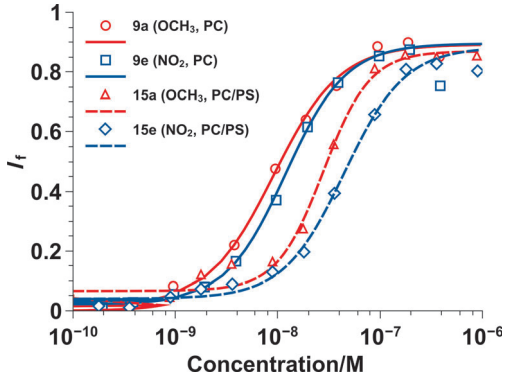

Figure 5. Homopolymer versus random copolymer Hill plots for π-rich polymers **9a** and **15a** (red) and π-poor polymers **9e** and **15e** (blue) using 100 nm PC/PS (80:20) large unilamellar vesicles swelled with carboxyfluorescein. Data was fit to the Hill Equation, and I_f represents the fraction of dye released. Solid lines represent diester homopolymers, and dashed lines represent random copolymers.

compare to their corresponding diester homopolymers for PC and PC/PS vesicles can be observed in Figures 4 and 5, respectively.

EC_{50} values for **14a**, **c**, and **e** were similar to those obtained for **9a**, **c**, and **e** when tested with PC vesicles and the overlays of the Hill plots in Figure 4 further suggest that there was little difference between the activity of the diester homopolymers and the less hydrophobic random copolymers. When tested with PC/PS vesicles, there was a slight increase in EC_{50} values for the random copolymers compared to the homopolymers, and there was a noticeable shift in the Hill plots in Figure 5. However, the shift was about the same for all diester random copolymers and thus attributed to the lower hydrophobic content and not due to the π-electronics of the system. Because no trend was observed, it was concluded that π electronics do not play a major role in CPPM activity. Alternatively, it is possible that the assay used herein does not have the fidelity to distinguish the subtleties of π interactions despite the fact that these same assays previously illustrated that adding hydrophobicity improves activity, with aromatic groups outperforming aliphatic groups.[6d,e] Even though we were able to synthesize a series of polymers that contained aromatic groups with an electrostatic potential range of −29.69 to 15.57 kcal mol^{-1}, it is also possible that the structural modifications made to the polymers may not have been significant enough to impact CPPM activity. Although it is likely that overall CPPM hydrophobicity and cationic charge are more influential design parameters than π-electronics, these results indicate that a wide range of aromatic groups can be incorporated into the polymer structures with limited impact on CPPM activity. From a design standpoint, this opens up additional ways in which CPPMs can be modified without inhibiting their performance.

Conclusion

For this study, aromatic groups containing electron-donating and electron-withdrawing groups were chemically incorporated into CPPM structures as a way to tune π interactions. It was hypothesized that tuning the quadrupole moments of the aromatic rings would provide additional control over CPPM activity. When synthesizing the monomers for these studies, it was established through small-molecule synthesis that highly electron-withdrawing groups could not be chemically incorporated into the diester versions of our oxanorbornene monomers, because it spontaneously induced a retro-Diels–Alder reaction.

Within the synthetically accessible series, vesicle-dye-release experiments were performed as a way to determine the CPPMs' EC_{50} values and assess their relative activities. It was shown by using PC vesicles that polymer backbone did not impact activity for the π-rich/π-poor CPPMs and that the electron-donating or electron-withdrawing groups, as well as the relative hydrophobic content did not impact activity either. Diester CPPMs were also tested with PC vesicles containing 20% PS anionic lipids in efforts to more thoroughly understand π-membrane interactions.

However, it would seem that only overall hydrophobicity dictated polymer activity and not the incorporated electron-donating or electron-withdrawing groups. Although it is possible that the assay used could not distinguish the subtleties of π interactions, it is also likely that the structural modifications made to the polymers were not significant enough to impact CPPM activity, despite the fact that molecules containing aromatic rings with an electrostatic potential range of −29.69 to +15.57 kcal mol^{-1} were explored. This suggests that other design parameters, such as overall hydrophobicity and cationic charge, have a greater impact on CPPM activity. The results also indicate that a wide range of aromatic groups can be incorporated into the polymer structures with limited impact on CPPM activity. This is encouraging from a design standpoint, because it expands potential functionality without impacting activity. Understanding these design principles will help to guide the development of future CPPMs.

Acknowledgements

The work was funded by the NIH (T32 GMO8515) and NSF (CHE-0910963). The authors would like to thank Dr. Hitesh D. Thaker, Dr. Jing Jiang, Prof. Ke Zhang, and Dr. Michael Lis for invaluable scientific discussions and help with half-ester and monomer purifications. The authors would also like to thank Ms. Catherine N. Walker, Mr. Ilker Ozay, and Mr. Nicholas Posey for their feedback on early drafts of this manuscript. Mass spectral data were obtained at the University of Massachusetts Mass Spectrometry Facility, which is supported in part by NSF.

Keywords: peptides · peptidomimetics · pi interactions · polymerization · proteins

[1] a) C. B. Cooley, B. M. Trantow, F. Nederberg, M. K. Kiesewetter, J. L. Hedrick, R. M. Waymouth, P. A. Wender, *J. Am. Chem. Soc.* **2009**, *131*, 16401; b) S. Futaki, T. Suzuki, W. Ohashi, T. Yagami, S. Tanaka, K. Ueda, Y. Sugiura, *J. Biol. Chem.* **2001**, *276*, 5836 – 5840; c) E. I. Geihe, C. B. Cooley, J. R. Simon, M. K. Kiesewetter, J. A. Edward, R. P. Hickerson, R. L. Kaspar, J. L. Hedrick, R. M. Waymouth, P. A. Wender, *Proc. Natl. Acad. Sci. USA* **2012**, *109*, 13171 – 13176; d) M. Lindgren, U. Langel, *Cell-Penetrating Peptides: Methods and Protocols* **2011**, *683*, 3 – 19; e) M. C. Morris, J. Depollier, J. Mery, F. Heitz, G. Divita, *Nat. Biotechnol.* **2001**, *19*, 1173 – 1176; f) J. B. Opalinska, A. M. Gewirtz, *Nat. Rev. Drug Discov.* **2002**, *1*, 503 – 514; g) L. N. Patel, J. L. Zaro, W. C. Shen, *Pharm. Res.* **2007**, *24*, 1977 – 1992; h) F. Sgolastra, B. M. deRonde, J. M. Sarapas, A. Som, G. N. Tew, *Acc. Chem. Res.* **2013**, *46*, 2977 – 2987; i) P. A. Wender, D. J. Mitchell, K. Pattabiraman, E. T. Pelkey, L. Steinman, J. B. Rothbard, *Proc. Natl. Acad. Sci. USA* **2000**, *97*, 13003 – 13008; j) C. Bechara, S. Sagan, *FEBS Lett.* **2013**, *587*, 1693 – 1702.

[2] a) A. Joliot, C. Pernelle, H. Deagostinibazin, A. Prochiantz, *Proc. Natl. Acad. Sci. USA* **1991**, *88*, 1864 – 1868; b) M. Green, P. M. Loewenstein, *Cell* **1988**, *55*, 1179 – 1188; c) A. D. Frankel, C. O. Pabo, *Cell* **1988**, *55*, 1189 – 1193.

[3] a) D. Derossi, A. H. Joliot, G. Chassaing, A. Prochiantz, *J. Biol. Chem.* **1994**, *269*, 10444 – 10450; b) S. Fawell, J. Seery, Y. Daikh, C. Moore, L. L. Chen, B. Pepinsky, J. Barsoum, *Proc. Natl. Acad. Sci. USA* **1994**, *91*, 664 – 668; c) E. Vives, P. Brodin, B. Lebleu, *J. Biol. Chem.* **1997**, *272*, 16010 – 16017.

[4] a) A. O. Tezgel, J. C. Telfer, G. N. Tew, *Biomacromolecules* **2011**, *12*, 3078 – 3083; b) L. C. Yin, H. Y. Tang, K. H. Kim, N. Zheng, Z. Y. Song, N. P. Gabrielson, H. Lu, J. J. Cheng, *Angew. Chem. Int. Ed.* **2013**, *52*, 9182 – 9186; *Angew. Chem.* **2013**, *125*, 9352 – 9356; c) N. P. Gabrielson, H. Lu, L. C. Yin, K. H. Kim, J. J. Cheng, *Mol. Ther.* **2012**, *20*, 1599 – 1609; d) H. Y. Tang, L. C. Yin, K. H. Kim, J. J. Cheng, *Chem. Sci.* **2013**, *4*, 3839 – 3844; e) E. G. Stanzl, B. M. Trantow, J. R. Vargas, P. A. Wender, *Acc. Chem. Res.* **2013**, *46*, 2944 – 2954; f) A. O. Tezgel, G. Gonzalez-Perez, J. C. Telfer, B. A. Osborne, L. M. Minter, G. N. Tew, *Mol. Ther.* **2013**, *21*, 201 – 209.

[5] a) S. Futaki, *Adv. Drug Delivery Rev.* **2005**, *57*, 547 – 558; b) A. Mishra, G. H. Lai, N. W. Schmidt, V. Z. Sun, A. R. Rodriguez, R. Tong, L. Tang, J. Cheng, T. J. Deming, D. T. Kamei, G. C. Wong, *Proc. Natl. Acad. Sci. USA* **2011**, *108*, 16883 – 16888; c) J. L. Zaro, W. C. Shen, *Exp. Cell Res.* **2005**, *307*, 164 – 173; d) P. E. Thorén, D. Persson, P. Isakson, M. Goksor, A. Onfelt, B. Norden, *Biochem. Biophys. Res. Commun.* **2003**, *307*, 100 – 107; e) T. Suzuki, S. Futaki, M. Niwa, S. Tanaka, K. Ueda, Y. Sugiura, *J. Biol. Chem.* **2002**, *277*, 2437 – 2443; f) T. Takeuchi, M. Kosuge, A. Tadokoro, Y. Sugiura, M. Nishi, M. Kawata, N. Sakai, S. Matile, S. Futaki, *ACS Chem. Biol.* **2006**, *1*, 299 – 303.

[6] a) A. Hennig, G. J. Gabriel, G. N. Tew, S. Matile, *J. Am. Chem. Soc.* **2008**, *130*, 10338 – 10344; b) N. Sakai, S. Matile, *J. Am. Chem. Soc.* **2003**, *125*, 14348 – 14356; c) N. W. Schmidt, M. Lis, K. Zhao, G. H. Lai, A. N. Alexandrova, G. N. Tew, G. C. Wong, *J. Am. Chem. Soc.* **2012**, *134*, 19207 – 19216; d) A. Som, A. Reuter, G. N. Tew, *Angew. Chem. Int. Ed.* **2012**, *51*, 980 – 983; *Angew. Chem.* **2012**, *124*, 1004 – 1007; e) A. Som, A. O. Tezgel, G. J. Gabriel, G. N. Tew, *Angew. Chem. Int. Ed.* **2011**, *50*, 6147 – 6150; *Angew. Chem.* **2011**, *123*, 6271 – 6274.

[7] a) F. Perret, M. Nishihara, T. Takeuchi, S. Futaki, A. N. Lazar, A. W. Coleman, N. Sakai, S. Matile, *J. Am. Chem. Soc.* **2005**, *127*, 1114 – 1115; b) M. Nishihara, F. Perret, T. Takeuchi, S. Futaki, A. N. Lazar, A. W. Coleman, N. Sakai, S. Matile, *Org. Biomol. Chem.* **2005**, *3*, 1659 – 1669; c) N. Sakai, S. Futaki, S. Matile, *Soft Matter.* **2006**, *2*, 636 – 641; d) N. Sakai, T. Takeuchi, S. Futaki, S. Matile, *ChemBioChem* **2005**, *6*, 114 – 122.

[8] a) P. F. Almeida, A. Pokorny, *Biochemistry* **2009**, *48*, 8083 – 8093; b) P. F. Almeida, A. Pokorny, *Methods Mol. Biol.* **2010**, *618*, 155 – 169.

[9] a) W. M. Yau, W. C. Wimley, K. Gawrisch, S. H. White, *Biochemistry* **1998**, *37*, 14713 – 14718; b) J. A. Killian, G. von Heijne, *Trends Biochem. Sci.* **2000**, *25*, 429 – 434.

[10] a) S. H. White, W. C. Wimley, *Annu. Rev. Biophys. Biomol. Struct.* **1999**, *28*, 319 – 365; b) W. C. Wimley, S. H. White, *Nat. Struct. Biol.* **1996**, *3*, 842 – 848.

[11] a) M. C. Morris, P. Vidal, L. Chaloin, F. Heitz, G. Divita, *Nucleic Acids Res.* **1997**, *25*, 2730 – 2736; b) M. C. Morris, S. Deshayes, F. Heitz, G. Divita, *Biol. Cell* **2008**, *100*, 201 – 217; c) C. E. Caesar, E. K. Esbjorner, P. Lincoln, B. Norden, *Biochemistry* **2006**, *45*, 7682 – 7692; d) H. Yezid, K. Konate, S. Debaisieux, A. Bonhoure, B. Beaumelle, *J. Biol. Chem.* **2009**, *284*, 22736 – 22746.

[12] a) G. J. Gabriel, J. G. Pool, A. Som, J. M. Dabkowski, E. B. Coughlin, M. Muthukumar, G. N. Tew, *Langmuir* **2008**, *24*, 12489 – 12495; b) H. D. Thaker, F. Sgolastra, D. Clements, R. W. Scott, G. N. Tew, *J. Med. Chem.* **2011**, *54*, 2241 – 2254.

[13] a) P. Braun, G. von Heijne, *Biochemistry* **1999**, *38*, 9778 – 9782; b) E. Strandberg, S. Morein, D. T. Rijkers, R. M. Liskamp, P. C. van der Wel, J. A. Killian, *Biochemistry* **2002**, *41*, 7190 – 7198; c) W. John Haynes, X. L. Zhou, Z. W. Su, S. H. Loukin, Y. Saimi, C. Kung, *FEBS Lett.* **2008**, *582*, 1514 – 1518; d) M. M. Gromiha, M. Suwa, *Int. J. Biol. Macromol.* **2005**, *35*, 55 – 62; e) M. M. Gromiha, *Biophys. Chem.* **2003**, *103*, 251 – 258; f) A. Arbuzova, L. Wang, J. Wang, G. Hangyas-Mihalyne, D. Murray, B. Honig, S. McLaughlin, *Biochemistry* **2000**, *39*, 10330 – 10339.

[14] K. Lienkamp, A. E. Madkour, A. Musante, C. F. Nelson, K. Nusslein, G. N. Tew, *J Am Chem. Soc* **2008**, *130*, 9836 – 9843.

[15] P. Nanjappan, A. W. Czarnik, *J. Org. Chem.* **1986**, *51*, 2851 – 2853.

[16] B. L. Schottel, H. T. Chifotides, K. R. Dunbar, *Chem. Soc. Rev.* **2008**, *37*, 68 – 83.

[17] Spartan '04, Wavefunction Inc., Irvine, CA, **2004**; software available at http://www.wavefun.com/products/spartan.html.

Received: September 23, 2014
Published online on December 23, 2014